European Journal of Mechanics B/Fluids 54 (2015) 69–81

Contents lists available at ScienceDirect

European Journal of Mechanics B/Fluids

journal homepage: www.elsevier.com/locate/ejmflu

Analytical solutions for two hollow vortex configurations in an infinite channel

Christopher C. Green

Department of Mechanical & Aerospace Engineering, University of California San Diego, 9500 Gilman Drive, La Jolla, CA 92023-0411, USA

ARTICLE INFO

Article history:
Received 6 February 2015
Received in revised form
12 May 2015
Accepted 30 June 2015
Available online 14 July 2015

In memory of Alan Elcrat

Keywords:
Hollow vortex
Channel
Free boundary problem
Free streamline theory
Conformal mapping
Schottky–Klein prime function

ABSTRACT

New analytical solutions for a co-travelling hollow vortex pair and a single row of hollow vortices in an infinite channel are presented. These new solutions generalise several known classical solutions for hollow vortices. The mathematical problems to be solved in each geometry are particular types of free boundary problem over a multiply connected domain. We present concise formulae for the conformal mapping determining the shape of the boundaries of the hollow vortices in both channel geometries by employing free streamline theory in combination with the function theory of the Schottky–Klein prime function. Various properties of the solutions are also presented.

1. Introduction

This paper is devoted to the solution of two free boundary problems concerning different configurations of hollow vortices set in the infinite channel geometry: a pair of steadily translating hollow vortices, and a single row of hollow vortices. We define a hollow vortex to be a finite-area region containing fluid at constant pressure having a non-zero circulation around it and situated in an otherwise irrotational flow. The hollow vortex model is a classical one, with the first works considering the model dating back to the late nineteenth century (Hicks [1], Michell [2], Pocklington [3]), and an example of a so-called 'distributed vorticity' model. Distributed vorticity models are desingularisations of the well-known point vortex model. Another example of a distributed vorticity model is that of the vortex patch which is a finite-area region of constant vorticity (Saffman [4]). By channel geometry, we mean a channel of infinite length with straight parallel walls containing inviscid and incompressible fluid. Since we will be modelling the fluid as inviscid and incompressible, we will be solving Laplace's equation in the channel geometries and determining the free boundary shapes of the hollow vortices.

One of the main goals of this paper is to employ special mathematical methods, centred around conformal mapping techniques and the function theory of the Schottky–Klein prime function, to reveal the families of boundary shapes of the hollow vortices in a particular configuration. The hollow vortex model has been of considerable interest in recent years and many analytical solutions describing hollow vortices in different configurations have recently been discovered: works worthy of a mention involving the hollow vortex model include, for example, [5–11]. In addition, Giannakidis [12] has undertaken a numerical study into the effects of placing a Sadovskii vortex (of which the hollow vortex is a special type) in a channel containing ideal fluid. The results of this paper will add to this growing body of work.

Two of the earliest works involving the hollow vortex model are directly relevant to the free boundary problems we shall tackle in this paper. The work of Michell [2] briefly examines the case of a single hollow vortex in an infinite channel of ideal fluid. Michell employed hodograph plane methods to derive an analytical formula, in terms of elliptic functions, for the shape of the free boundary. An interesting feature of this configuration is that the hollow vortex is stationary for all time and does not propagate along the channel. Pocklington [3] found solutions for a steadily translating pair of hollow vortices in unbounded ideal fluid. Pocklington also utilised hodograph plane methods and elliptic functions to derive an analytical solution for the free boundaries of the hollow vortices. For this configuration, the pair of hollow vortices translates at constant speed parallel to their axis of symmetry, without change of form.

E-mail address: ccgreen@ucsd.edu.

http://dx.doi.org/10.1016/j.euromechflu.2015.06.013
0997-7546/

Baker, Saffman & Sheffield [13] studied a single row of hollow vortices in unbounded fluid. A row refers to an infinite line of equally-separated hollow vortices of equal circulation, and is an example of a configuration of hollow vortices which remains in equilibrium for all time. For a row of hollow vortices in a channel, an equilibrium will also be attained provided the centroids of the hollow vortices are aligned along the channel centreline. With hodograph methods again proving to be fruitful, Baker, Saffman & Sheffield [13] found an exact solution describing the shapes of hollow vortices aligned in a single row in unbounded fluid by appealing to the intrinsic periodic structure of the row. Crowdy & Green [5] have also presented an equivalent exact solution for the row of hollow vortices in unbounded fluid in an arguably more concise mathematical form. In this paper, we will make connections with, and offer generalisations of, all three of these classical solutions due to Michell [2], Pocklington [3], and Baker, Saffman & Sheffield [13].

Recently, Crowdy, Llewellyn Smith & Freilich [7] have presented a new derivation and representation of Pocklington's solution [3] for a co-travelling hollow vortex pair. Their approach was to use free streamline theory to establish solutions for the conformal mapping determining the hollow vortex boundary shapes. Another recent study by Zannetti & Lasagna [11] replaces the stagnation points associated with hollow vortex pairs by so-called 'Chaplygin cusps', or finite-area regions of stagnant fluid at constant pressure. Through the use of hodograph plane techniques, Zannetti & Lasagna [11] have been able to determine analytical formulae for a pair of hollow vortices in an infinite channel, in terms of elliptic functions, but their approach is conceptually different from ours. Zannetti & Lasagna's solution for a hollow vortex pair in a channel arises from their analysis of Chaplygin cusps with the latter not appearing explicitly in their solutions. In the present paper, we will offer a different approach to obtaining these solutions, an approach which should be emphasised has also been very successful in producing other hollow vortex solutions; for example, in [5,7,9].

The configurations of hollow vortices in the infinite channel geometry we shall consider herein are examples of so-called 'wall-bounded flows'. They are the solutions to particular free boundary problems set in multiply connected domains: the hollow vortex boundaries are unknown *a priori* and must be determined as part of the solution. As such, the configurations are expected to exhibit interesting physical features as well as requiring a special mathematical treatment. This special mathematical treatment essentially involves the utilisation of the function theory of the Schottky–Klein prime function; in particular, the usage of particular types of conformal slit mappings. An accessible review of this function theory is given by Crowdy [14], and a survey of where it has been used to solve various applied mathematical problems in multiply connected geometries is given in Crowdy [15]. As in [15], the analytical solutions we will construct in this paper advocate these conformal slit mappings as important 'building block' functions for the construction of functions which must exhibit certain desired properties in a particular multiply connected domain. An important contribution of this paper is the resolution of two challenging free boundary problems through the use of novel mathematical methods. These problems both turn out to have analytical solutions which can be neatly expressed as indefinite integrals whose integrands are written in terms of Schottky–Klein prime functions. This paper emphasises the demonstration of these novel mathematical methods in producing hollow vortex solutions.

In this paper, the function theory of the Schottky–Klein prime function will be combined, in a natural way, with ideas from free streamline theory. We will perform our analysis in a parametric ζ-plane by finding separate conformal mapping expressions for the complex potential $W(\zeta)$ and the complex velocity function $(dw/dz)(\zeta)$ corresponding to a particular hollow vortex configuration. The chain rule then allows us to construct an integral for the conformal map $z(\zeta)$ we ultimately seek determining the shapes of the hollow vortex free boundaries, i.e.:

$$z(\zeta) = \int_{\zeta_0}^{\zeta} \frac{(dW/d\zeta)(\zeta')}{(dw/dz)(\zeta')} d\zeta'. \tag{1.1}$$

This same approach was adopted, for example, in [5,7,9]. We will see again in this paper that using free streamline theory is a particularly advantageous approach given that formulae for $W(\zeta)$ and $(dw/dz)(\zeta)$ can be constructed in a straightforward manner using the function theory to be introduced herein.

The remainder of this paper is laid out as follows. We will first provide an overview of the relevant conformal slit mappings which we will use to construct our solutions in Section 2. In Sections 3 and 4, we will separately formulate and solve the two aforementioned free boundary problems and obtain analytical solutions for the hollow vortices. For both hollow vortex configurations, we will present several families of hollow vortex solution-shapes, and examine some of their key characteristics, which are summarised and discussed in Section 5.

2. Conformal slit mappings

We will now introduce three types of conformal slit mapping which will be used to construct our solutions, and whose analytical formulae are given in terms of the Schottky–Klein prime function. Further details on these important conformal mappings can be found in Crowdy & Marshall [16], and for conciseness, we will only present the bare essentials here. Throughout, let $\omega(\zeta, \gamma)$ denote the Schottky–Klein prime function associated with a *given* $M + 1$ connected circular domain D_ζ which, for us, will consist of the bounded region in a parametric ζ-plane between the unit circle and M smaller excised circles lying within it. The reader is referred to Green [17] for a more detailed presentation of the relevant function theory of the Schottky–Klein prime function, and to the works of Crowdy and collaborators mentioned therein. The relevant form of the Schottky–Klein prime function will be given at the beginning of the following two sections.

Let us first introduce the circular slit mapping

$$\eta(\zeta; \gamma) = \frac{\omega(\zeta, \gamma)}{|\gamma|\omega(\zeta, 1/\overline{\gamma})} \tag{2.1}$$

where $\gamma \in \mathbb{C}$ is an arbitrary point in D_ζ. $\eta(\zeta; \gamma)$ has a simple zero at $\zeta = \gamma$. This function $\eta(\zeta, \gamma)$ maps the unit circle $|\zeta| = 1$ onto another unit circle $|\eta| = 1$ and maps each of the interior circles onto finite-length concentric circular slits lying in the interior of $|\eta| = 1$. It also has the property that $|\eta(\zeta; \gamma)| =$ constant on each boundary circle of D_ζ.

Let us now introduce the radial slit mapping

$$\chi(\zeta; \alpha, \beta) = \frac{\omega(\zeta, \alpha)\omega(\zeta, 1/\overline{\alpha})}{\omega(\zeta, \beta)\omega(\zeta, 1/\overline{\beta})} \tag{2.2}$$

where $\alpha, \beta \in \mathbb{C}$ are arbitrary points in D_ζ. $\chi(\zeta; \alpha, \beta)$ has a simple zero at $\zeta = \alpha$ and a simple pole at $\zeta = \beta$. This function $\chi(\zeta; \alpha, \beta)$ maps each boundary circle of D_ζ onto finite-length radial slits emanating from the origin. It also has the property that $\arg[\chi(\zeta; \alpha, \beta)] =$ constant on each boundary circle of D_ζ.

Finally, we shall introduce another kind of radial slit mapping:

$$\xi(\zeta; 1, -1) = \frac{\omega(\zeta, 1)}{\omega(\zeta, -1)}. \tag{2.3}$$

$\xi(\zeta; 1, -1)$ has a simple zero at $\zeta = 1$ and a simple pole at $\zeta = -1$. This function $\xi(\zeta; 1, -1)$ maps the unit circle $|\zeta| = 1$ onto a vertical straight line through the origin in the ξ-plane and

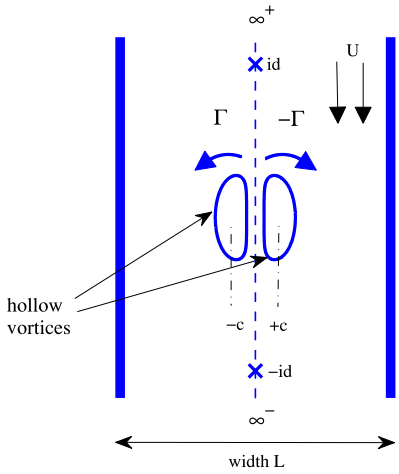

Fig. 1. Schematic, in a co-travelling frame moving with the hollow vortices, of an infinite channel containing a pair of hollow vortices of equal and opposite circulation. The centroids of the hollow vortices are taken to be such that $\mathrm{Re}[z] = \pm c$. The two stagnation points are indicated by crosses. The two ends of the channel at infinity are denoted by $\infty^{\pm}$. The shapes of the hollow vortex boundaries are to be determined.

maps each of the interior circles of D_ζ onto finite-length horizontal slits each lying along the negative real ξ-axis.

3. Hollow vortex pair in an infinite channel

In this section, we solve the free boundary problem associated with a co-travelling pair of hollow vortices in an infinite channel. From a physical viewpoint, one question fuelling the present study is how introducing a distributed vorticity structure into a confined geometry has an effect on the shape of its free boundary. We are also motivated in devising an idealised mathematical model of a vortex ring travelling along a pipe: the two-dimensional analogue of this problem is precisely the free boundary problem now being examined. The solutions we present in this section could therefore be viewed as a complement to a recent experimental study by Stewart et al. [18], where particle image velocimetry was used to study the evolution of vortex ring circulation in a channel. Furthermore, our solutions could also be used in a simple mathematical model of a cardiovascular flow since it is well-known that vortical structures can form in the ventricles of the heart (see, for example, [19,20]).

3.1. Schottky–Klein prime function

The Schottky–Klein prime function, up to a pre-multiplicative constant, associated with the concentric annulus $\rho < |\zeta| < 1$, is given by the following infinite product:

$$\omega(\zeta, \gamma) = P(\zeta/\gamma, \rho) = (1 - \zeta/\gamma)\prod_{j=1}^{\infty}(1 - \rho^{2j}\zeta/\gamma)(1 - \rho^{2j}\gamma/\zeta). \tag{3.1}$$

$P(\zeta/\gamma, \rho)$ is an analytic function everywhere in $\rho < |\zeta| < 1$. Introduce also the function

$$K(\zeta, \rho) = \frac{\zeta P'(\zeta, \rho)}{P(\zeta, \rho)} \tag{3.2}$$

where $P'(\zeta, \rho)$ denotes the derivative of $P(\zeta, \rho)$ with respect to the first argument. Note that $K(\zeta, \rho)$ has simple poles at $\zeta = \rho^{2n}$, $n \in \mathbb{Z}$ (i.e. at the simple zeroes of $P(\zeta, \rho)$).

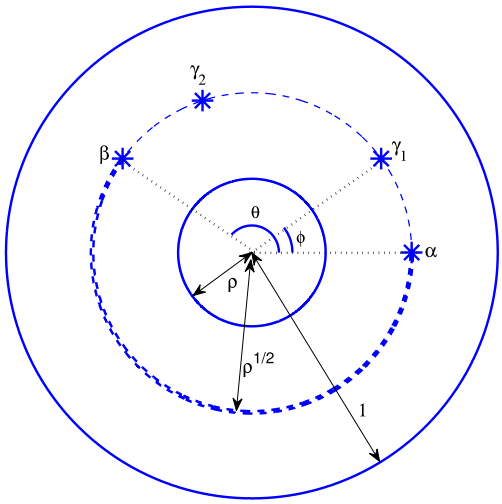

Fig. 2. Schematic of the preimage circular domain in the ζ-plane. The circles $|\zeta| = 1$ and $|\zeta| = \rho$ map to the two hollow vortex boundaries under the map $z(\zeta)$. The branch cut joining $\zeta = \alpha$ and $\zeta = \beta$ (the preimages of $\infty^{\pm}$) on $|\zeta| = \sqrt{\rho}$ is shown as a double-dashed line. The preimages of the two stagnation points on $|\zeta| = \sqrt{\rho}$ are labelled by $\zeta = \gamma_1$ and $\zeta = \gamma_2$.

3.2. Formulation of the problem

In a physical $z = (x + \mathrm{i}y)$-plane, consider an infinite channel of width L filled with inviscid, incompressible and irrotational fluid with impenetrable walls at $x = \pm L/2$. We will seek solutions for which a hollow vortex pair is steadily translating along the channel in the y-direction with speed U. We will focus on solutions yielding a hollow vortex pair which have equal area and which are symmetric about the channel centreline. In a co-travelling frame of reference, one hollow vortex is assumed to have its centroid at $x = c$ and to have circulation $-\Gamma$ (where $\Gamma > 0$) with the other hollow vortex assumed to have its centroid at $x = -c$ with circulation Γ. Fig. 1 shows a schematic of this configuration.

Consider a conformal mapping $z(\zeta)$ from a concentric annulus $\rho < |\zeta| < 1$ to the fluid region occupying the infinite channel exterior to the two hollow vortices. Let the circles $|\zeta| = 1$ and $|\zeta| = \rho$ map to the two hollow vortex boundaries in the channel. Let the two points $\zeta = \alpha$ and $\zeta = \beta$ lying inside this concentric annulus map to the two ends of the channel at infinity which we shall label by $\infty^{\pm}$. This means that we require

$$z(\zeta) = \frac{\mathrm{i}L}{2\pi}\log(\zeta - \alpha) + \text{locally analytic function}, \quad \zeta \to \alpha, \tag{3.3}$$

and

$$z(\zeta) = -\frac{\mathrm{i}L}{2\pi}\log(\zeta - \beta) + \text{locally analytic function}, \quad \zeta \to \beta. \tag{3.4}$$

It will be necessary to make some choice of branch cut between the two logarithmic branch points at $\zeta = \alpha$ and $\zeta = \beta$, and it is natural to choose this so that the images under $z(\zeta)$ of the two sides of the branch cut map to the channel walls. The choice of this branch cut will be made later. Fig. 2 shows a schematic of the preimage domain in the ζ-plane.

The reason for choosing to map the two sides of the branch cut onto the channel walls becomes apparent if we consider an equivalent problem. If, instead of considering an infinite channel containing a pair of hollow vortices, we consider a singly periodic array of period windows (each extending to $y = \infty^{\pm}$ and each containing a pair of hollow vortices), the problem now has an intrinsic periodicity structure and is analogous to the mathematical

framework introduced by Crowdy & Green [5] in their study of von Kármán streets of hollow vortices. The two problems are equivalent because, in the infinite channel case, the channel walls are streamlines, whilst in the singly periodic case, the straight vertical edges of a typical period window are precisely the same streamlines. For the case of the pair of hollow vortices in a channel, there is no periodicity in the problem, but when interpreted as a singly periodic array of hollow vortex pairs in free space, we can view the two sides of the branch cut mapping to the edges of a typical period window or, equivalently, the two channel walls.

3.3. Function $W(\zeta)$

We shall work in the co-travelling frame with the hollow vortex pair in which the configuration is steady. Let the complex potential associated with the flow in the co-travelling frame be $w(z)$. Introduce the composition

$$W(\zeta) = w(z(\zeta)). \tag{3.5}$$

The circulations around the two hollow vortices are $\pm\Gamma$; this means that

$$\oint_{|\zeta|=1} d[W(\zeta)] = -\oint_{|\zeta|=\rho} d[W(\zeta)] = -\Gamma, \tag{3.6}$$

where both $|\zeta| = 1$ and $|\zeta| = \rho$ are positively oriented in the anticlockwise direction. As $z \to \infty^{\pm}$, we require

$$w(z) = \mathrm{i}Uz + \text{locally analytic function}. \tag{3.7}$$

Apart from this simple pole at infinity, $w(z)$ is an analytic function everywhere in the fluid region exterior to the two hollow vortices. In light of (3.3), (3.4) and (3.7), we require

$$W(\zeta) = -\frac{LU}{2\pi}\log(\zeta-\alpha) + \text{locally analytic function}, \ \zeta \to \alpha, \tag{3.8}$$

and

$$W(\zeta) = \frac{LU}{2\pi}\log(\zeta-\beta) + \text{locally analytic function}, \ \zeta \to \beta. \tag{3.9}$$

The function $W(\zeta)$ must also satisfy

$$\mathrm{Im}[W(\zeta)] = \text{constant} \tag{3.10}$$

on both circles $|\zeta| = 1$ and $|\zeta| = \rho$, as well as on the two sides of the branch cut, thereby ensuring that the two hollow vortex boundaries *and* the two channel walls are streamlines of the flow.

We claim that the function $W(\zeta)$ is

$$W(\zeta) = -\frac{\mathrm{i}\Gamma}{2\pi}\log\zeta - \frac{LU}{2\pi}\log\chi(\zeta;\alpha,\beta), \tag{3.11}$$

where $\chi(\zeta;\alpha,\beta)$ is the radial slit mapping of (2.2). Due to the presence of $\chi(\zeta;\alpha,\beta)$ in (3.11), (3.10) is clearly satisfied on $|\zeta| = 1$ and $|\zeta| = \rho$. It also has the required behaviours (3.8) and (3.9) near $\zeta = \alpha$ and $\zeta = \beta$. It changes by Γ as either $|\zeta| = 1$ or $|\zeta| = \rho$ is traversed in an anticlockwise sense thereby producing the required circulations (3.6) around the hollow vortices. We may choose $\zeta = \alpha$ to be on the positive real axis by the remaining rotational freedom of the Riemann–Koebe mapping theorem and, in order to enforce the required left–right symmetry about the vertical channel centreline, we take

$$\alpha = \sqrt{\rho}. \tag{3.12}$$

Then

$$\beta = \sqrt{\rho}\mathrm{e}^{\mathrm{i}\theta} \tag{3.13}$$

where $\theta \in \mathbb{R}$ will need to be determined.

3.4. Function $(dw/dz)(\zeta)$

The complex velocity function needs to be analytic and single-valued in the fluid region exterior to the two hollow vortices. Based on the problem of a co-travelling point vortex pair in an infinite channel (see Appendix), we expect two stagnation points at $z = \pm\mathrm{i}d$ where $d \in \mathbb{R}$ is to be determined (see Fig. 1); this implies that the preimages of this pair of stagnation points will lie on $|\zeta| = \sqrt{\rho}$. Thus dw/dz will have two simple zeroes:

$$\frac{dw}{dz}(\gamma_1) = \frac{dw}{dz}(\gamma_2) = 0. \tag{3.14}$$

Here, the preimages of the two stagnation points have been labelled by $\zeta = \gamma_1$ and $\zeta = \gamma_2$. To ensure continuity of pressure across the hollow vortex boundaries, Bernoulli's theorem implies that the fluid speed on the hollow vortex boundaries must be constant. Thus, we require

$$\left|\frac{dw}{dz}\right| = \text{constant} \tag{3.15}$$

on both $|\zeta| = 1$ and $|\zeta| = \rho$. We also require dw/dz to be L-periodic across the channel.

We claim that the function $(dw/dz)(\zeta)$ is

$$\frac{dw}{dz} = \frac{R\eta(\zeta;\gamma_1)\eta(\zeta;\gamma_2)}{\zeta}. \tag{3.16}$$

Here, $R \in \mathbb{C}$ is a constant and $\eta(\zeta;\gamma)$ is the circular slit mapping of (2.1). This function (3.16) has constant modulus on $|\zeta| = 1$ and $|\zeta| = \rho$, and two simple zeroes at $\zeta = \gamma_1$ and $\zeta = \gamma_2$, as required. It is analytic and single-valued in $\rho < |\zeta| < 1$ and so it is invariant as either $\zeta = \sqrt{\rho}$ or $\zeta = \beta$ is encircled, and hence L-periodic across the channel. The factor of ζ in the denominator of (3.16) can be explained as follows. Note from (3.11) that $W_\zeta(\zeta)$ has a simple pole at $\zeta = 0$. In order that $z_\zeta(\zeta)$ not have a simple pole at $\zeta = 0$, and thereby be appropriately single-valued upon traversing either $|\zeta| = 1$ or $|\zeta| = \rho$ (for particular values of $\zeta = \gamma_1$ and $\zeta = \gamma_2$ to be determined), it is required that $(dw/dz)(\zeta)$ must indeed have a simple pole at $\zeta = 0$.

The parameters $\zeta = \gamma_1$ and $\zeta = \gamma_2$ are two solutions in $\rho < |\zeta| < 1$ of the equation

$$\frac{dW}{d\zeta}(\zeta) = 0, \tag{3.17}$$

which, on use of (3.2) and (3.11), can be expressed as

$$K(\gamma_j/\sqrt{\rho},\rho) + K(\gamma_j\sqrt{\rho},\rho) - K(\gamma_j/\beta,\rho) - K(\gamma_j\overline{\beta},\rho) = -\frac{\mathrm{i}\Gamma}{LU}, \quad j = 1,2. \tag{3.18}$$

Since

$$\frac{dw}{dz} \to \mathrm{i}U, \quad z \to \infty^{\pm}, \tag{3.19}$$

we must have

$$\frac{R\eta(\alpha;\gamma_1)\eta(\alpha;\gamma_2)}{\alpha} = \frac{R\eta(\beta;\gamma_1)\eta(\beta;\gamma_2)}{\beta} = \mathrm{i}U. \tag{3.20}$$

One of the equations in (3.20) can be used to determine the value of R; the velocity field then follows from (3.16) once a particular choice of branch cut between $\zeta = \sqrt{\rho}$ and $\zeta = \beta$ is made. This choice of branch cut is discussed later.

3.5. Conformal map $z(\zeta)$

By using arguments akin to those presented by Crowdy & Green [5], it can be shown that the function $\zeta W_\zeta(\zeta)$ is a loxodromic function, and furthermore, it can be argued that another representation of $\zeta W_\zeta(\zeta)$ is given by

$$\zeta W_\zeta(\zeta) = \mathcal{B}\frac{P(\zeta/\gamma_1,\rho)P(\zeta\overline{\gamma_1},\rho)P(\zeta/\gamma_2,\rho)P(\zeta\overline{\gamma_2},\rho)}{P(\zeta/\sqrt{\rho},\rho)P(\zeta\sqrt{\rho},\rho)P(\zeta/\beta,\rho)P(\zeta\overline{\beta},\rho)}, \quad (3.21)$$

where $\mathcal{B}\in\mathbb{C}$ is a constant. By the chain rule, it follows on use of (3.16) and (3.21) that

$$\frac{dz}{d\zeta} = \mathcal{A}\frac{P^2(\zeta\overline{\gamma_1},\rho)P^2(\zeta\overline{\gamma_2},\rho)}{P(\zeta/\sqrt{\rho},\rho)P(\zeta\sqrt{\rho},\rho)P(\zeta/\beta,\rho)P(\zeta\overline{\beta},\rho)}, \quad (3.22)$$

where $\mathcal{A}\in\mathbb{C}$ is a constant. Thus, an integral for the conformal mapping $z(\zeta)$ is

$$z(\zeta) = \mathcal{A}\int_{\zeta_0}^{\zeta}\frac{P^2(\zeta'\overline{\gamma_1},\rho)P^2(\zeta'\overline{\gamma_2},\rho)}{P(\zeta'/\sqrt{\rho},\rho)P(\zeta'\sqrt{\rho},\rho)P(\zeta'/\beta,\rho)P(\zeta'\overline{\beta},\rho)}d\zeta'. \quad (3.23)$$

Here, $\zeta_0\in\mathbb{C}$ is an arbitrary point inside the annulus $\rho<|\zeta|<1$. The value of the pre-multiplicative constant $\mathcal{A}$ in (3.23) is found *a posteriori* by insisting that the residue of $dz/d\zeta$ at $\zeta=\sqrt{\rho}$ is $iL/2\pi$ as required by (3.3). An explicit expression for it is given by

$$\mathcal{A} = -\frac{iL}{2\pi}\left(\frac{\hat{P}(1,\rho)P(\rho,\rho)P(\sqrt{\rho}/\beta,\rho)P(\sqrt{\rho}\overline{\beta},\rho)}{\sqrt{\rho}P^2(\sqrt{\rho}\overline{\gamma_1},\rho)P^2(\sqrt{\rho}\overline{\gamma_2},\rho)}\right), \quad (3.24)$$

where

$$\hat{P}(\zeta,\rho) = \frac{P(\zeta,\rho)}{1-\zeta}. \quad (3.25)$$

3.6. Characterisation of the solutions

We will now examine several properties of the solutions. We fix

$$L = \Gamma = 1. \quad (3.26)$$

This corresponds, respectively, to setting the length and the time scale of the problem. The analogous problem of a pair of point vortices in an infinite channel admits a one-parameter family of solutions (see Appendix); we shall take this parameter to be $c\in\mathbb{R}$, where the centroids of the two hollow vortices are

$$x = \pm c. \quad (3.27)$$

We additionally expect to be able to dictate the area of the hollow vortices, and a natural way to do this is to specify the value of ρ. Once all the parameters have been determined, the translation speed U of the hollow vortices follows from (3.18):

$$U = \left[i\left(K(\gamma_1/\sqrt{\rho},\rho)+K(\gamma_1\sqrt{\rho},\rho)-K(\gamma_1/\beta,\rho)-K(\gamma_1\overline{\beta},\rho)\right)\right]^{-1}. \quad (3.28)$$

The constant ζ_0 in the conformal map (3.23) reflects a translational degree of freedom which can be set arbitrarily and the mapping shifted by an appropriate constant *a posteriori*. We shall now proceed to examine the solution class with c and ρ as our two free real parameters.

Our general strategy in finding solutions is to choose a value c for the hollow vortex centroids and then gradually increase the value of ρ from zero in a standard continuation procedure. We have found that solutions for a hollow vortex pair of equal area and which are symmetric about the channel centreline are given by the special parameter choices:

$$\beta = \sqrt{\rho}e^{i\theta}, \quad \gamma_1 = \sqrt{\rho}e^{i\phi}, \quad \gamma_2 = \frac{\sqrt{\rho}\beta}{\gamma_1} = \sqrt{\rho}e^{i(\theta-\phi)}. \quad (3.29)$$

Fig. 2 shows the location of these parameters (3.29) in the preimage ζ-plane. With these parameter choices (3.29), the images of the circles $|\zeta|=1$ and $|\zeta|=\rho$ under the map (3.23) are reflections of each other through the channel centreline. For given values of ρ and c, the two real parameters

$$\theta = \arg[\beta], \qquad \phi = \arg[\gamma_1], \quad (3.30)$$

remain to be determined. One condition to determine these parameters is

$$\mathrm{Re}\left[\oint_{|\zeta|=1} z_\zeta(\zeta')d\zeta'\right] = 0 \quad (3.31)$$

which is a necessary condition for the image of $|\zeta|=1$ under $z(\zeta)$ to be a closed curve. Once (3.31) has been satisfied, the symmetry is such that the image of $|\zeta|=\rho$ is also a closed curve. The other condition to be enforced is

$$\mathrm{Re}\left[\oint_{|\zeta|=\rho} z(\zeta')|z_\zeta(\zeta')d\zeta'|\right] \Big/ \left(\oint_{|\zeta|=\rho}\left|z_\zeta(\zeta')d\zeta'\right|\right) = c. \quad (3.32)$$

This sets the real part of one of the hollow vortex centroids. Eqs. (3.31) and (3.32) can be readily solved using Newton's method.

It is important to note that thus far, we have not enforced the streamline conditions (3.10) on the channel walls. Indeed, we have not even determined the preimages of the channel walls in the ζ-plane. We will now show that the channel walls correspond to the image of an arc of the circle $|\zeta|=\sqrt{\rho}$ under the conformal mapping $z(\zeta)$. It can be shown that

$$\mathrm{Im}[W(\zeta)] = \text{constant} \quad (3.33)$$

on $|\zeta|=\sqrt{\rho}$. Recall that $\zeta=\sqrt{\rho}$ and $\zeta=\beta$ map to the two ends of the channel at $\infty^{\pm}$. In view of the left–right symmetry of the configuration in the z-plane, one arc of the circle $|\zeta|=\sqrt{\rho}$ between $\zeta=\sqrt{\rho}$ and $\zeta=\beta$ will map onto the channel centreline $x=0$ joining $\infty^{\pm}$. The preimages of the stagnation points, $\zeta=\gamma_1$ and $\zeta=\gamma_2$, will lie on this arc. (3.33) then immediately implies that the channel centreline $x=0$ will indeed be a streamline of the flow, as required. The second arc on $|\zeta|=\sqrt{\rho}$ joining $\zeta=\sqrt{\rho}$ and $\zeta=\beta$ will be taken to be our branch cut whose two sides will map to the channel walls (see Fig. 2). It is then automatic from (3.33) that the two channel walls will indeed be streamlines of the flow, as required.

Figs. 3 and 4 show infinite channels of unit width containing co-travelling hollow vortex pairs of varying area. In each channel, the hollow vortex centroids are fixed at $\mathrm{Re}[z]=\pm c$, for some specified value of c. We have established that there exist solutions, each corresponding to a particular shape of hollow vortex, for all values of ρ. One interesting observation to make is that our solutions do not exhibit maximum area configurations; rather, the area of the hollow vortices appears to increase without bound as $\rho\to 1$. This is consistent with the results shown in Fig. 6 which shows graphs of hollow vortex area as a function of ρ: the area of the hollow vortices, for a given value of c, is a monotonically increasing function of ρ. We observe that the hollow vortex areas are smallest when the centroids are closest together, and are largest when the centroids are equi-distant to the channel centreline and to a channel wall. For small values of ρ, the hollow vortices are always found to be small and almost circular. We also remark that the hollow vortices in figures two and six of Zannetti & Lasagna [11] look qualitatively the same as our solutions for similar hollow vortex areas and centroid locations; this is reassuring given that our mathematical approaches are different.

Pocklington [3] notes that when a pair of co-travelling hollow vortices in free space is very close together, their boundary shapes are much flatter on their near rather than on their remote sides. We observe this phenomenon when $c=\pm 1/16$ and $c=\pm 1/8$

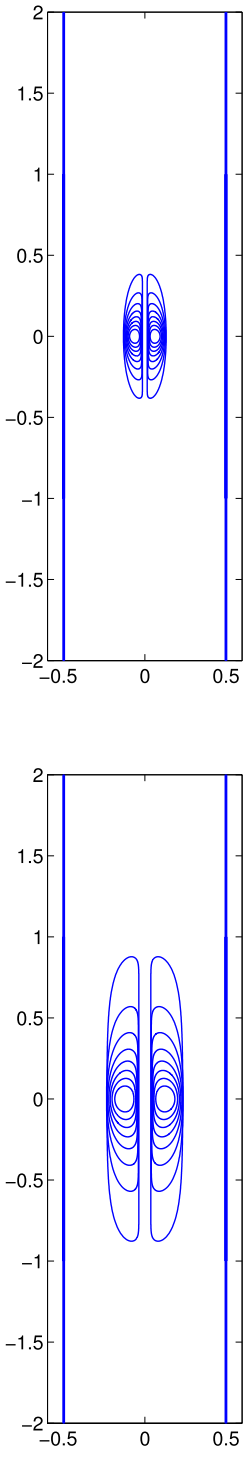

Fig. 3. Superposition of co-travelling hollow vortex pairs in an infinite channel of unit width with centroids $c = \pm 1/16$ (left) and $c = \pm 1/8$ (right).

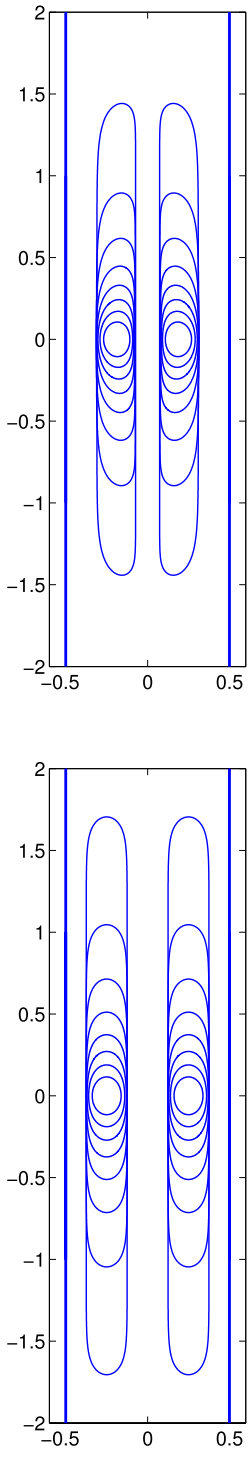

Fig. 4. Superposition of co-travelling hollow vortex pairs in an infinite channel of unit width with centroids $c = \pm 3/16$ (left) and $c = \pm 1/4$ (right). The solutions for $c = \pm 1/4$ correspond to the solutions due to Michell [2].

in Fig. 3, when the centroids are close together. These hollow vortex shapes indeed closely resemble those found by Pocklington [3]; this is to be expected when the centroids are close together because the hollow vortices are never close to the channel walls and should therefore appear qualitatively similar to their free space counterparts. Indeed, our solutions can be viewed as generalisations of the co-travelling hollow vortex pair due to Pocklington [3] to the infinite channel geometry.

The case when $c = \pm 1/4$ is special (see Fig. 4). Here, the two centroids of the hollow vortex pair are equi-distant to both the channel centreline and to one of the channel walls. Since the channel centreline *and* the channel walls are streamlines of the flow, the hollow vortex shapes in the case when $c = \pm 1/4$ are precisely those obtainable from the solution due to Michell [2] for a single hollow vortex in an infinite channel. It should be possible to exactly superpose a solution of given area, obtained from the conformal map in [2], onto one of our solutions with the same area. However, due to a lack of notational explanation in Michell's paper, we have been unable to do this.

We have also established that both the area and the centroid locations have an effect on the speed of translation of the hollow

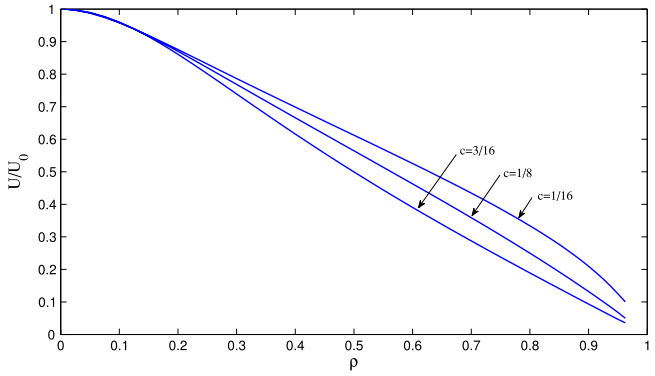

Fig. 5. Graphs, for three different hollow vortex centroids, of the quantity U/U_0 as a function of ρ. As expected, each graph tends to unity in the limit as $\rho \to 0$.

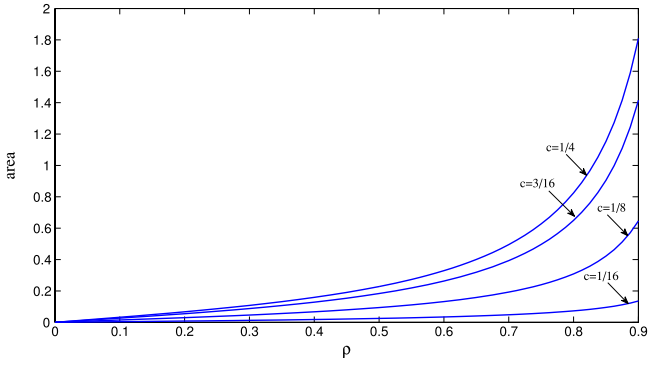

Fig. 6. Graphs, for four different hollow vortex centroids, of hollow vortex area as a function of ρ. As $\rho \to 1$, the area of the hollow vortices grows without bound.

vortex pair along the channel. Fig. 5 shows graphs of the ratio U/U_0 as a function of ρ, where U_0 is the speed of translation of a pair of point vortices with circulations ± 1 in an infinite channel positioned at $\mathrm{Re}[z] = \pm c$:

$$U_0 = \frac{1}{2}\cot(2\pi c). \tag{3.34}$$

The graph for $c = 1/4$ does not feature because the hollow vortex pair in this case is stationary for all time (recall the single hollow vortex considered by Michell [2] is also stationary for all time). For each value of c, it is clear that

$$\lim_{\rho \to 0} \frac{U}{U_0} = 1 \tag{3.35}$$

as expected. For a fixed value of c, we observe that U is a monotonically decreasing function with hollow vortex area: hollow vortex pairs with larger areas will translate with smaller speeds. We also observe that the hollow vortex pairs whose centroids are closest together move along the channel faster than those pairs whose centroids are spaced further apart.

4. Row of hollow vortices in an infinite channel

We shall now consider the case of a single row of hollow vortices, whose centroids are aligned along the channel centreline, in an infinite channel. In doing so, we will be considering generalisations of the works of both Michell [2] and Baker, Saffman & Sheffield [13]. Recall that by a row of hollow vortices, we mean an infinite line of equally-separated hollow vortices of equal circulation.

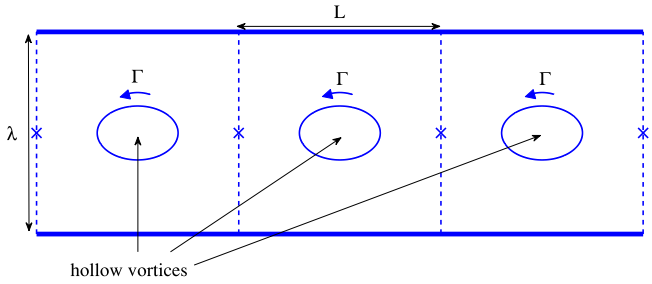

Fig. 7. Schematic showing three periods of length L of a row of hollow vortices, each of circulation Γ, in an infinite channel of width λ in a z-plane. The horizontal channel walls are $\mathrm{Im}[z] = \pm y = \lambda/2$. Each of the hollow vortex centroids in this row lie on the channel centreline $\mathrm{Im}[z] = 0$. Stagnation points are indicated by crosses. The shapes of the hollow vortex boundaries are to be determined.

4.1. Schottky–Klein prime function

One form of the Schottky–Klein prime function is presented in Baker [21]:

$$\omega(\zeta, \gamma) = (\zeta - \gamma) \prod_{\theta \in \Theta''} \{\zeta, \theta(\zeta), \gamma, \theta(\gamma)\}. \tag{4.1}$$

Here, the brace notation denotes the cross-ratio, and Θ'' is a particular subset of the Schottky group Θ associated with a bounded $M+1$ connected planar circular domain D_ζ. $\omega(\zeta, \gamma)$ is an analytic function everywhere in D_ζ. For present purposes, it should be thought of as a special computable function and can be accurately computed using software based on the numerical algorithm presented in Green [17].

Associated with D_ζ (and hence with $\omega(\zeta, \gamma)$) is the set of M integrals of the first kind $\{v_j(\zeta) \mid j = 1, \ldots, M\}$. These are multi-valued analytic functions everywhere in D_ζ with

$$\mathrm{Im}[v_j(\zeta)] = 0, \ \zeta \in C_0, \ \mathrm{Im}[v_j(\zeta)] = \gamma_{jk}, \ \zeta \in C_k, k = 1, \ldots, M, \tag{4.2}$$

where $\gamma_{jk} \in \mathbb{R}$ are constants, and

$$\oint_{C_j} d[v_k(\zeta)] = \delta_{jk}, \tag{4.3}$$

where δ_{jk} denotes the Kronecker delta function. Again, the reader is referred to [17] and the references therein for further detail on these functions.

4.2. Formulation of problem

In a physical $z = (x + \mathrm{i}y)$-plane, consider a horizontal parallel-sided channel whose two ends extend to infinity in both directions and which has a width λ. Let the impenetrable walls of the channel be the horizontal lines $y = \pm\lambda/2$ so that the channel centreline is $y = 0$. Let the centroids of the hollow vortices be located at $x = nL$, $n \in \mathbb{Z}$, so that L be the period of the configuration i.e. the horizontal length between two neighbouring hollow vortex centroids on the channel centreline. Let the circulation of each of the hollow vortices in the row be Γ. These hollow vortices in the row are expected to remain in equilibrium for all time. Given this periodic structure, it suffices to consider a single period cell of the configuration: this cell contains one hollow vortex of finite-area with circulation Γ, and has the dimensions $L \times \lambda$. Fig. 7 illustrates this arrangement.

Let D_ζ be the following triply connected bounded circular domain in a parametric ζ-plane. Let the unit ζ-circle be labelled C_0. Take the unit ζ-disc and from it excise two smaller discs whose boundaries are the circles C_1 and C_2. Let the centre of C_1 be $-\delta$ and

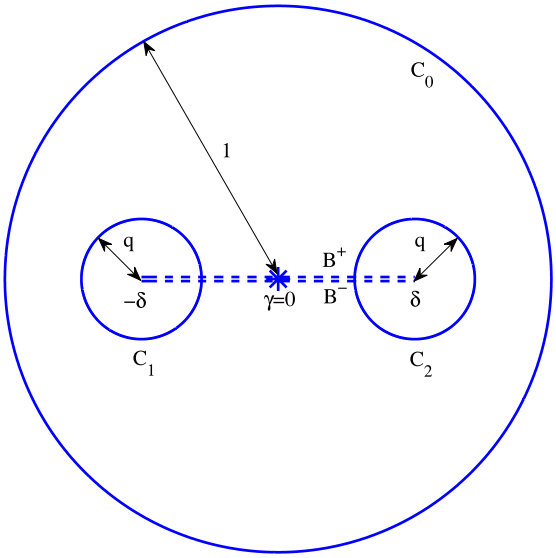

Fig. 8. Schematic showing the preimage triply connected bounded circular domain D_ζ in the ζ-plane. Under the conformal map $z(\zeta)$, the unit circle C_0 is taken to map to the hollow vortex boundary and the two interior circles C_1 and C_2 are taken respectively to map to the top and bottom horizontal channel walls of the period cell. The branch cut joining the centres of C_1 and C_2 is shown as a double-dashed line. The two sides of this branch cut $B^\pm$ lying in the interior of D_ζ map to the two vertical edges of the period cell.

let the centre of C_2 be δ, where $\delta \in \mathbb{R}$. Owing to the up–down symmetry of the period cell about the channel centreline, let the radius of both C_1 and C_2 be q. Fig. 8 shows a schematic of D_ζ in this case. In choosing this preimage domain D_ζ, we have used up the three real degrees of freedom associated with the Riemann–Koebe mapping theorem.

Consider a conformal mapping $z(\zeta)$ taking the interior of D_ζ to a single period cell of the hollow vortex row in the channel. Our task is to determine the shape of the boundary of the hollow vortex in this period cell. Let the unit circle C_0 be mapped onto the boundary of the hollow vortex in the period cell, and let the interior circles C_1 and C_2 be mapped onto the top and bottom horizontal channel walls of the period cell. Note that traversing C_0 in an anticlockwise sense corresponds to traversing the boundary of the hollow vortex in a clockwise sense.

In order to capture the periodic structure of the row of hollow vortices in the channel, and uniquely define the conformal map $z(\zeta)$, we must make a choice of branch cut in D_ζ. Since C_1 and C_2 map to the two channel walls of the period cell, the branch cut must link these two circles. The two sides of this branch cut, lying in the interior of D_ζ, will map to the two straight vertical edges of the period cell. A 2π traversal of either C_1 or C_2 corresponds to moving a distance L along a channel wall; encircling C_1 or C_2 by more than 2π corresponds to moving a distance L along the wall and into the neighbouring period cell. In light of this, it is natural to take the branch cut along the real axis through the origin, joining the centres of C_1 and C_2 between $\zeta = -\delta$ and $\zeta = \delta$.

Rosenhead [22] has analysed von Kármán point vortex streets in an infinite channel. From Rosenhead's work, we are led to expect two stagnation points lying on the vertical edges of each of our period cells. Moreover, we expect both these stagnation points to lie on the channel centreline. In light of this, we expect the same point in D_ζ, lying on the branch cut, to map to both stagnation points. Let the preimage in D_ζ of these two stagnation points be labelled $\zeta = \gamma \in \mathbb{R}$. For hollow vortices whose centroids lie on the channel centreline, it is clear from the symmetry that $\gamma = 0$ (see Fig. 8).

4.3. Function $W(\zeta)$

Let the complex potential for the flow associated with the hollow vortex row in the channel be denoted by $w(z)$. We need the total circulation in the period cell to be Γ:

$$\oint_{\partial D} d[w(z)] = \Gamma. \tag{4.4}$$

Here, we let ∂D denote the boundary of the period cell, i.e. the two horizontal walls *and* the two vertical edges, and is positively oriented in the anticlockwise direction. Introducing the composition

$$W(\zeta) = w(z(\zeta)), \tag{4.5}$$

we see that in the ζ-plane, the integral (4.4) is

$$\oint_{C_1+B^++C_2+B^-} d[W(\zeta)] = \Gamma. \tag{4.6}$$

Here, B^+ denotes the top-side of the branch cut lying in the interior of D_ζ and B^- denotes the under-side. There is a net zero contribution to this integral as both sides of the branch cut are traversed owing to the opposite directions of integration. Consequently, the non-zero contribution to the integral in (4.6) must come from integrating around the circles C_1 and C_2: recall the properties of the $v_j(\zeta)$ functions (4.3) which allow us to fulfil this requirement. We also require the two channel walls and the hollow vortex boundary to be streamlines:

$$\mathrm{Im}[W(\zeta)] = \text{constant} \tag{4.7}$$

for $\zeta \in C_0, C_1, C_2$.

We propose the following function for the complex potential:

$$W(\zeta) = \frac{\Gamma}{2}\left(v_1(\zeta) + v_2(\zeta)\right). \tag{4.8}$$

Given the up–down symmetry of the period cell about the channel centreline, we would expect an equal contribution to the total circulation in the period cell from each of the two channel walls; this explains the pre-multiplying constant $\Gamma/2$. It follows from the properties (4.3) that (4.8) indeed satisfies (4.6). From the properties (4.2), (4.8) is easily seen to have constant imaginary part on each of the boundary circles of D_ζ. Taking a derivative of (4.8) with respect to ζ yields

$$\frac{dW}{d\zeta}(\zeta) = \frac{\Gamma}{2}\left(v_1'(\zeta) + v_2'(\zeta)\right). \tag{4.9}$$

Here, $v_j'(\zeta)$ means the derivative of $v_j(\zeta)$ with respect to ζ. (4.9) is required to have a simple zero at $\zeta = 0$. Let us show that this is in fact the case. The properties (4.3) of the $v_j(\zeta)$ functions imply that

$$v_j(\zeta) = \frac{1}{2\pi \mathrm{i}} \log(\zeta - \delta_j) + \text{locally analytic function}, \ j = 1, \ldots, M. \tag{4.10}$$

Differentiating (4.10) with respect to ζ implies

$$v_j'(\zeta) = \frac{1}{2\pi \mathrm{i}} \frac{1}{\zeta - \delta_j} + c_j + \text{locally analytic function}, \ j = 1, \ldots, M, \tag{4.11}$$

where $c_j \in \mathbb{C}$ are constants. In the present case, we have $\delta_1 = -\delta$ and $\delta_2 = \delta$. Note that as $\zeta \to 0$, it follows from (4.11) that

$$v_1'(\zeta) = \frac{1}{2\pi \mathrm{i}\delta} + c_1 + \text{locally analytic function} \tag{4.12}$$

and

$$v_2'(\zeta) = -\frac{1}{2\pi \mathrm{i}\delta} + c_2 + \text{locally analytic function}, \tag{4.13}$$

where $c_1, c_2 \in \mathbb{C}$ are constants. But, given the symmetry of D_ζ, it turns out that $c_1 = -c_2$. Thus, the simple zero of $dW/d\zeta$ at $\zeta = 0$ is intrinsic in (4.9).

4.4. Function dw/dz

Bernoulli's theorem implies that the fluid speed must be constant on the boundary of the hollow vortex:

$$\left|\frac{dw}{dz}(\zeta)\right| = Q_0, \quad \zeta \in C_0. \tag{4.14}$$

Here, $Q_0 \in \mathbb{R}$ is a positive constant. The fluid velocity $u - \mathrm{i}v$ on the two channel walls must be purely tangential to the walls; that is, the fluid velocity is purely real on the two channel walls:

$$v = -\mathrm{Im}\left[\frac{dw}{dz}(\zeta)\right] = 0, \quad \zeta \in C_1, C_2. \tag{4.15}$$

We need dw/dz to have a simple zero at $\zeta = 0$ in order to include the two stagnation points:

$$\frac{dw}{dz}(0) = 0. \tag{4.16}$$

We also require dw/dz to be L-periodic in the x-direction (i.e. the fluid velocity is equal on the two vertical edges of the period cell).

In order to construct the complex velocity function, we appeal to a special class of conformal mappings known as polycircular arc mappings. The target domains of these maps are multiply connected regions whose boundaries consist of a union of circular arc segments. Consider the following polycircular arc mapping:

$$\mathcal{S}(\zeta; R) = \frac{\omega(\zeta, -1) - R\omega(\zeta, 1)}{\omega(\zeta, -1) + R\omega(\zeta, 1)}, \tag{4.17}$$

where $R \in \mathbb{C}$ is a constant to be determined shortly. This conformal map can be constructed through the following composition:

$$\mathcal{S}(\zeta; R) = \mathcal{S}_2(\mathcal{S}_1(\zeta; R)), \tag{4.18}$$

where

$$\mathcal{S}_1(\zeta; R) = R\xi(\zeta; 1, -1), \qquad \mathcal{S}_2(\zeta) = \frac{1-\zeta}{1+\zeta}, \tag{4.19}$$

and $\xi(\zeta; 1, -1)$ is the radial slit mapping (2.3).

The function $\mathcal{S}(\zeta; R)$ maps C_0 to the unit $\mathcal{S}$-circle with C_1 and C_2 mapping to two finite-length horizontal slits lying on the real axis. Fig. 9 shows a schematic of this triply connected polycircular arc domain. Fig. 10 shows a schematic of the sequence of conformal maps (4.19) required to map D_ζ, as in Fig. 8, to the polycircular arc domain as in Fig. 9. Further details on the construction of conformal mappings to multiply connected polycircular arc domains can be found in Crowdy, Fokas & Green [23].

We claim that the complex velocity function is

$$\frac{dw}{dz} = Q_0\mathcal{S}(\zeta; R) = Q_0\left[\frac{\omega(\zeta, -1) - R\omega(\zeta, 1)}{\omega(\zeta, -1) + R\omega(\zeta, 1)}\right]. \tag{4.20}$$

Note that the conditions (4.15) are automatically satisfied by this function (4.20) given the nature of the image of D_ζ under the polycircular arc mapping (4.17), i.e. the triply connected polycircular arc domain shown in Fig. 9. The condition (4.14) is clearly satisfied. Notice that this mapping (4.20) has a simple zero at $\zeta = 0$ if we choose

$$R = \frac{\omega(0, -1)}{\omega(0, 1)}, \tag{4.21}$$

thus satisfying (4.16). Function (4.20) is also analytic and single-valued everywhere in the interior of D_ζ and hence dw/dz is L-periodic across the period cell.

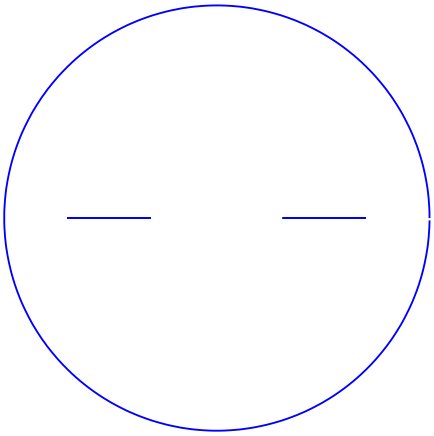

Fig. 9. Schematic showing the image of D_ζ (as in Fig. 8) under the polycircular arc mapping $\mathcal{S}(\zeta; R)$ given in (4.17). Under this map, C_0 is mapped onto the unit circle whilst C_1 and C_2 are mapped onto two finite-length horizontal slits on the real axis.

4.5. Conformal map $z(\zeta)$

By free streamline theory, the conformal map determining the shape of the boundary of the hollow vortex in a typical period window, with centroid on the channel centreline, is given through the integral

$$z(\zeta) = \frac{\Gamma}{2Q_0}\int_{\zeta_0}^{\zeta} \frac{v_1'(\zeta') + v_2'(\zeta')}{\mathcal{S}(\zeta'; R)}d\zeta' = \frac{\Gamma}{2Q_0}\int_{\zeta_0}^{\zeta} \left(v_1'(\zeta') + v_2'(\zeta')\right) \times \left[\frac{\omega(\zeta', -1) + R\omega(\zeta', 1)}{\omega(\zeta', -1) - R\omega(\zeta', 1)}\right]d\zeta' \tag{4.22}$$

where $\zeta_0 \in \mathbb{C}$ is an arbitrary point in the interior of D_ζ, and R is as in (4.21).

4.6. Characterisation of the solutions

We will now look at some of the properties exhibited by the solutions. Let us set the length scale and the time scale of the problem by fixing

$$L = \Gamma = 1. \tag{4.23}$$

Let us define the aspect ratio of the period cell to be $\mathcal{R} = \lambda/L$ so that, with $L = 1$, the aspect ratio of the period cell is

$$\mathcal{R} = \lambda. \tag{4.24}$$

We expect to be able to fix this aspect ratio of the period cell. As usual, the constant ζ_0 in the conformal map (4.22) reflects a translational degree of freedom which can be set arbitrarily and the mapping shifted by an appropriate constant *a posteriori*. The area associated with the hollow vortex can be assigned through the parameter q. We shall now proceed to examine the solution class with q as our only free parameter. This leaves just one real parameter, namely δ, to be found in order to determine the shape of the hollow vortex boundary in a typical period cell of the row.

Our general strategy in finding solutions is to choose a value of the aspect ratio λ and then gradually vary the value of q in a standard continuation procedure, solving for the value of δ in each case. Recall the preimage circular domain D_ζ in the ζ-plane. The centres of C_1 and C_2 are $\pm\delta \in \mathbb{R}$, and their radii are both q. We can choose this value of q *a priori*; this is analogous to fixing the area of the hollow vortex. We are then left with just the real parameter δ to determine. This is done by enforcing the single real condition prescribing the aspect ratio of the period cell:

$$\mathcal{R} = \left(\int_{-\delta+q}^{\delta-q} |z_\zeta(\zeta')d\zeta'|\right) \Big/ \left(\oint_{C_1} |z_\zeta(\zeta')d\zeta'|\right). \tag{4.25}$$

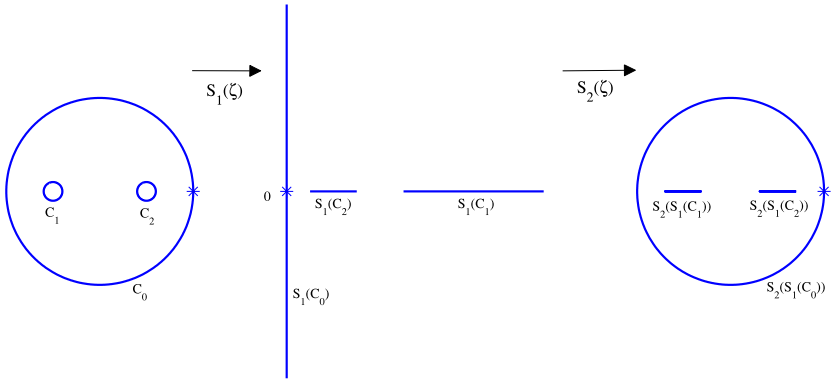

Fig. 10. Schematic showing the sequence of conformal mappings (4.19) for the construction of an analytical expression for the triply connected polycircular arc domain shown in Fig. 9.

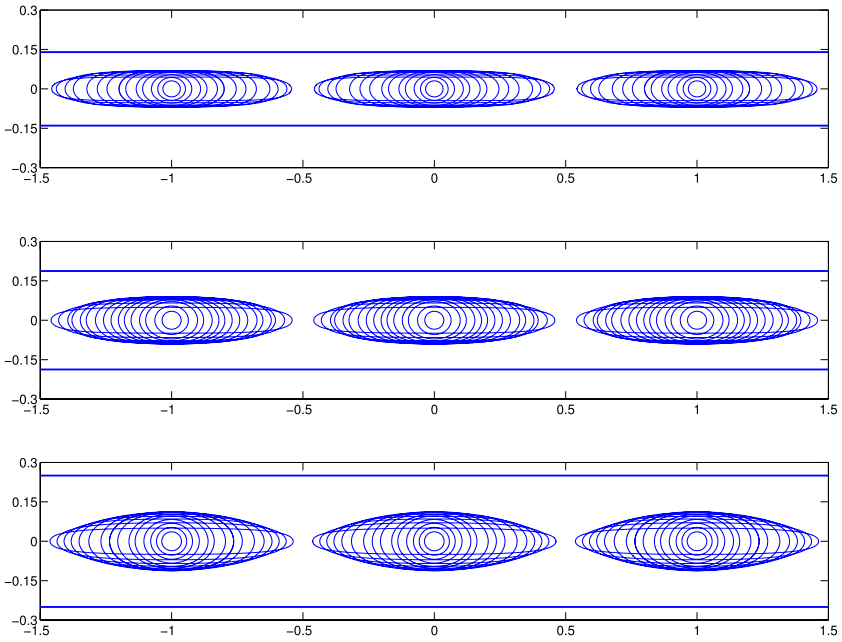

Fig. 11. Superposition of typical members of the hollow vortex row in an infinite channel, of varying area, for three different channel widths: $\lambda = 0.28$ (top), $\lambda = 0.375$ (centre) and $\lambda = 0.5$ (bottom). Three periods (of unit length $L = 1$) of the row are shown. For each λ, there is a hollow vortex with some maximum area.

(4.25) is readily solved by Newton's method. Owing to the up–down symmetry of the period cell about the channel centreline, the conformal map turns out to be automatically single-valued. It was checked that the image of C_0 under $z(\zeta)$ is indeed a closed curve, i.e.

$$\oint_{C_0} z_\zeta(\zeta')d\zeta' = 0. \tag{4.26}$$

From the value of δ found by solving (4.25), we can calculate the length, $\hat{L}$ (say), of one of the channel walls:

$$\hat{L} = \oint_{C_1} |z_\zeta(\zeta')d\zeta'|. \tag{4.27}$$

Then we can find the value of the pre-multiplicative constant in (4.22) *a posteriori*; this can be thought of as a rescaling parameter in order to fulfil our requirement that $L = 1$:

$$\frac{\Gamma}{2Q_0} = \frac{1}{\hat{L}}. \tag{4.28}$$

For a given area of the hollow vortex, we find that for any given channel width λ, there are two different pairs of values of δ and q defining the preimage domain D_ζ. These two pairs of conformal moduli correspond to hollow vortices exhibiting two different shapes but having the same area.

Fig. 11 shows three period cells making up three infinite channels with widths $\lambda = 0.28, 0.375$ and 0.5, respectively. In each period cell is a superposition of typical hollow vortex members, of different areas, forming part of the row in the channel. For each channel width, we observe that the hollow vortices vary in shape between one which is almost circular to one with long flattened faces along the two regions of their boundary which are closest to the channel walls. It is reassuring to observe that the hollow vortex shapes closely resemble those in free space (obtained either by using the conformal map presented in [5] or by using the solution in [13]) when the width of the channel becomes large; such hollow vortices are shown in Fig. 13 for $\lambda = 1$. These observations are consistent with the behaviour of the graphs shown in Fig. 14. Although not immediately apparent in Figs. 11 and 13, the graphs in Fig. 14 also confirm that there exists a unique hollow vortex shape of some maximum area for a given channel width. Fig. 12 compares one shape of hollow vortex, all of the same area, in three different channels with widths $\lambda = 0.25, 0.375$ and 0.5. The free space hollow vortex is superposed on each. It is seen that there is a noticeable difference in shape compared with the free space hollow vortex for small channel widths $\lambda \lesssim 0.375$, but when

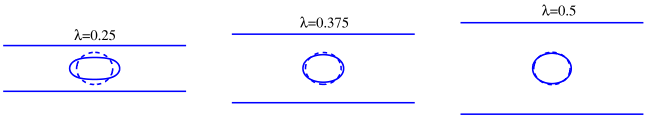

Fig. 12. Three plots, for channel widths $\lambda = 0.25$ (left), $\lambda = 0.375$ (centre) and $\lambda = 0.5$ (right), of typical hollow vortex members in a row, of area 0.027. Superposed for comparison is a Baker, Saffman & Sheffield [5] hollow vortex in free space also of area 0.027; these are shown as dashed lines. As the channel widens, our solutions tend towards the free space shapes.

$\lambda \approx 0.5$, the hollow vortex shapes assume essentially the same shapes as those in free space. Our solutions can be viewed as the generalisation of the free space hollow vortex row solutions due to Baker, Saffman & Sheffield [13] to the case of an infinite channel of finite width, and are also the singly periodic generalisations of the Michell [2] hollow vortex in an infinite channel.

Fig. 14 shows graphs, each corresponding to a different channel width λ, of the hollow vortex perimeter P as a function of inverse separation between the hollow vortex centroids L, each rescaled by the square root of the hollow vortex area A. Both of these quantities $P/A^{1/2}$ and $A^{1/2}/L$ (with $L = 1$) are dimensionless. Fig. 3 in Baker, Saffman & Sheffield [13] shows a graph of the same quantities for the single row of hollow vortices in free space: this graph is displayed in Fig. 14 by a dashed line. One observation to make is that for each channel width λ, there is a maximum value of $A^{1/2}$ that can be attained, and this occurs at a unique value of $P/A^{1/2}$. As λ is reduced, this maximum value of $A^{1/2}$ is also reduced, but the unique value of $P/A^{1/2}$ for which this is attained increases. For $\lambda = 1$, the maximum $A^{1/2} \approx 0.375$ and this is very close to the value for a single row of hollow vortices in free space which is $A^{1/2} \approx 0.38$ as reported by Baker, Saffman & Sheffield [13]: this is expected since $\lambda = 1$ corresponds to a wide channel. For $\lambda = 0.375$, the maximum $A^{1/2} \approx 0.33$, and for $\lambda = 0.28$, the maximum $A^{1/2} \approx 0.3$.

We observe that each of the graphs turn around on themselves implying non-uniqueness of the solutions for a given value of the area A and channel width λ; that is to say, for a given area A and channel width λ, there will be two possible hollow vortex shapes with the same area. There will exist two possible shapes provided the value of $A^{1/2}$ is less than the maximum possible value; there do not exist any solutions for a given channel width λ if one specifies an area greater than this permissible maximum. For a fixed area not close to the maximum, it appears that the hollow vortex with the higher value of $P/A^{1/2}$ exhibits a boundary shape with two elongated faces, whilst the hollow vortex with the lower value of $P/A^{1/2}$ appears to exhibit a quasi-elliptical or quasi-circular shape. For each channel width λ, the graphs each tend towards the free space graph when $A^{1/2} \to 0$ and when $P/A^{1/2} \to \infty$. When $A^{1/2} \to 0$, the hollow vortices are tending towards their point vortex counterparts by assuming near circular shapes of small

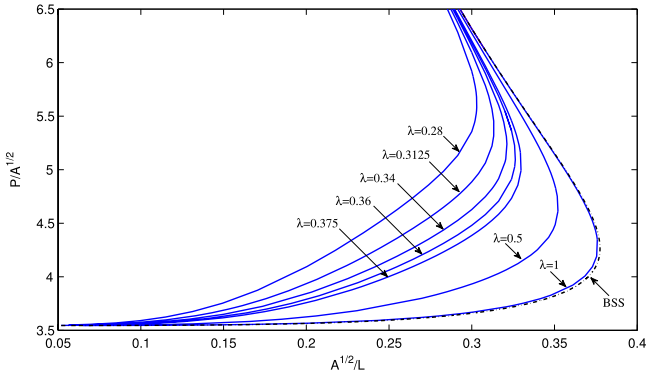

Fig. 14. Graphs, for seven different channel widths λ, of the quantity $P/A^{1/2}$ as a function of $A^{1/2}/L$ (with $L = 1$ fixed). Here, A and P denote the perimeter and area of the hollow vortex, respectively, and L denotes the separation between hollow vortex centroids. The corresponding graph for a single row of hollow vortices in free space is shown by the dashed line (labelled 'BSS').

area. Quantity $P/A^{1/2}$ has the minimum value $2\sqrt{\pi}$ for circles and each graph tends precisely to this value as $A^{1/2} \to 0$. As $P/A^{1/2} \to \infty$, the graphs will eventually intersect the vertical axis at infinity; this again corresponds to zero area solutions. The nature of these limiting shapes is of particular interest. As reported in Baker, Saffman & Sheffield [13], as $P/A^{1/2} \to \infty$ in free space, the result is a vortex sheet of constant strength. Our results seem to suggest that the same phenomenon occurs in channels; that is, for any channel width λ, it is expected that a vortex sheet of constant strength will form along the channel centreline as the hollow vortex area shrinks to zero from its maximum value.

It is important to note that the vertical axis in Fig. 14 has been deliberately truncated at $P/A^{1/2} = 6.5$ since beyond this point, for all the solution branches, accurate computation of the Schottky–Klein prime function becomes very difficult. This is because the inner circles C_1 and C_2 of the preimage circular domain become close to the unit circle C_0, and such domains pertain to the hollow vortices which are very close to one another at an edge between two neighbouring period windows. Also, for channel widths $\lambda \leq 0.28$, the radii of C_1 and C_2 become rather large, and again, accurate computation of the Schottky–Klein prime function becomes more challenging. Consequently, we stopped reducing the size of the channel widths at $\lambda = 0.28$. All the solution branches in Fig. 14 were terminated when convergence of the Newton iteration became hard to achieve. The shapes of all our computed hollow vortices do not exhibit any singularities, and all are univalent.

Finally, it is worth describing how the preimage circular domain D_ζ changes as the hollow vortex shapes vary in qualitative appearance, for a given channel width λ. The inner circles C_1 and C_2 are initially centred in the vicinity of the origin with small

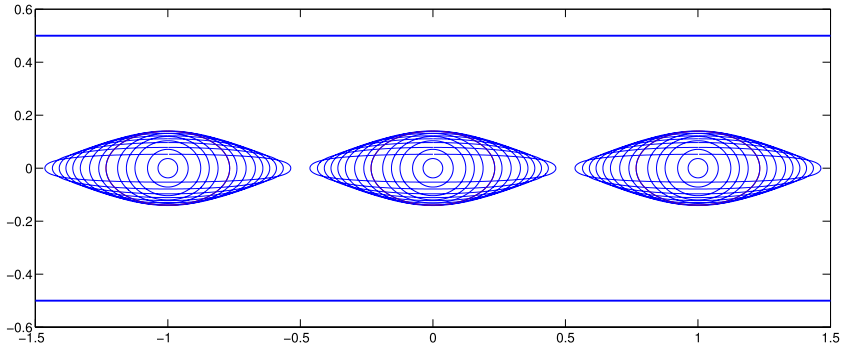

Fig. 13. Superposition of typical members of the hollow vortex row, of varying area, in an infinite channel of width $\lambda = 1$. Three periods (of unit length $L = 1$) of the row are shown. These hollow vortices essentially share the same shapes as hollow vortices in a row in free space.

radii; these domains correspond to small circular hollow vortices. C_1 and C_2 then gradually increase in radii and move apart until a maximum radius q is reached at some value of δ; this domain corresponds to the quasi-elliptical hollow vortices (note that this maximum radius q does not correspond to the maximum area hollow vortex). C_1 and C_2 continue moving apart, but with their radii now decreasing, until they get very close to the unit circle C_0; these domains correspond to the hollow vortices impinging on their neighbours.

5. Discussion

In this paper, we have presented closed-form analytical solutions to two free boundary problems involving hollow vortex configurations, sharing the common feature that they are both set in an infinite channel containing ideal fluid. We determined the free boundary shapes for a hollow vortex pair and for a single row of hollow vortices in an infinite channel. Incorporating the channel walls into the mathematical model (which are themselves *not* free boundaries) in addition to the free boundaries of the hollow vortices, required a delicate consideration of how the boundary conditions were to be enforced. The judicious combination of free streamline theory with conformal mapping techniques allowed us to solve the free boundary problems for the shapes of the hollow vortex boundaries which, as in other recent works (e.g. [5,7,9]), proved to be an expedient approach when modelling configurations of multiple hollow vortices.

In the case of the hollow vortex pair in an infinite channel, we determined the free boundary shapes by constructing a conformal mapping from the interior of a concentric annulus to the fluid region exterior of the hollow vortex pair with some choice of branch cut mapping to the two channel walls. The use of both radial and circular conformal slit maps proved to be crucial in constructing a concise integral formula for this conformal map (3.23). We established that both the area and the relative position of the hollow vortex pair to the channel side walls has an effect on the speed of translation in the channel, as well as on their shapes. Connections with two classical works were also made. Our solutions can be considered as generalisations to the infinite channel geometry of the solutions due to Pocklington [3]. When the centroids of the hollow vortex pair were equi-distant to the channel centreline and to one of the channel walls, we obtained the stationary solutions due to Michell [2]. Our analytical solutions for the co-travelling hollow vortex pair in an infinite channel also complement those analytical solutions found recently by Zannetti & Lasagna [11].

To determine the boundary shapes for hollow vortices arranged in a single row in an infinite channel, we restricted attention to a period cell containing a typical member of the row, with centroid on the channel centreline, and incorporated the periodic nature of the problem by introducing a branch cut in the preimage circular domain whose two sides were required to map to the vertical edges of the cell. We found a concise formula for the conformal map as an explicit indefinite integral to the interior of this period cell from a particular triply connected bounded circular domain. In devising this conformal map (4.22), we made use of the integrals of the first kind $v_j(\zeta)$ associated with the preimage domain and a special choice of polycircular arc mapping. Our solutions are natural generalisations to an infinite channel of the hollow vortex row solutions in free space due to Baker, Saffman & Sheffield [13]; our solutions are also the singly periodic generalisations of the single hollow vortex in an infinite channel due to Michell [2]. Three interesting discoveries were made for a given channel width: there exist two possible hollow vortex shapes for a given value of area; there exists a boundary shape with a maximum obtainable area; and the formation of a vortex sheet of constant strength is theoretically possible as the maximum area shape is deformed to zero area in a particular limit. Our approach to the single row in an infinite channel should be able to be readily generalised to the case where the centroids of the hollow vortices are not necessarily aligned along the channel centreline.

The new hollow vortex solutions of this paper should facilitate a study into the effect of compressibility on the two configurations by the performance of a low Mach number weakly compressible analysis via Rayleigh–Jansen expansions; our new hollow vortex solutions would be expected to be the leading order terms in these expansions. Ardalan, Meiron & Pullin [24] have examined the effects of compressibility on the structure of the single hollow vortex row by taking the Baker, Saffman & Sheffield [13] solution as the leading order term in their Rayleigh–Jansen expansion. Our new solutions should also enable a study into establishing the stability properties of the two configurations we have considered. Indeed, it should be possible to adapt the linear stability analyses presented in [7,9] to the new hollow vortex solutions presented in this paper. Luzzatto-Fegiz & Williamson [25] have presented a fascinating investigation using energy-based stability arguments into the possible equilibrium flows, and their associated stability properties, for von Kármán streets of finite-area vortex patches. A natural extension to the results in this paper would be to find analytical solutions describing a von Kármán street of hollow vortices in an infinite channel. Analytical solutions of this particular free boundary problem will offer an inviscid wake structure model in a confined environment, and will be couched in a rich mathematical structure. This problem presents several mathematical challenges, not least because of the intrinsic periodicity structure and a typical period window being quadruply connected.

Acknowledgements

The author acknowledges helpful discussions with Darren Crowdy, and the late Alan Elcrat to whom this work is dedicated. He wishes to thank the referees for their constructive comments. He also acknowledges financial support from a Lindemann Trust Fellowship of the English-Speaking Union in the UK.

Appendix

In this appendix, we outline the analysis for a pair of point vortices steadily translating along an infinite channel with vertically-aligned walls.

The complex potential for two point vortices with circulations $\pm\Gamma$ inside the unit circle in a parametric ζ-plane is

$$W(\zeta) = -\frac{\mathrm{i}\Gamma}{2\pi}\log\left(\frac{\zeta-\gamma_1}{\zeta-1/\overline{\gamma}_1}\right) + \frac{\mathrm{i}\Gamma}{2\pi}\log\left(\frac{\zeta-\gamma_2}{\zeta-1/\overline{\gamma_2}}\right). \tag{A.1}$$

The conformal mapping from an infinite vertical channel of unit width in a z-plane to the interior of the unit ζ-disc is given by

$$\zeta(z) = \tanh\left(\frac{\pi z}{2\mathrm{i}}\right). \tag{A.2}$$

Suppose the point vortices are located at

$$x = \pm c. \tag{A.3}$$

Their corresponding images in the ζ-plane are

$$\zeta = \pm\tanh(\pi c/2\mathrm{i}). \tag{A.4}$$

It follows, after some algebra, that the complex potential in the z-plane is

$$w(z) = -\frac{\mathrm{i}\Gamma}{2\pi}\log\left(\frac{\tanh(\mathrm{i}\pi z)+\tanh(\mathrm{i}\pi c)}{\tanh(\mathrm{i}\pi z)-\tanh(\mathrm{i}\pi c)}\right). \tag{A.5}$$

After some further algebra, it can be verified that the vortex pair travels along the channel with velocity

$$\frac{dw}{dz} = U - \mathrm{i}V = -\frac{\mathrm{i}\Gamma}{2}\cot(2\pi c). \tag{A.6}$$

When $c < 1/4$, the stagnation points are complex conjugate pairs lying on the channel centreline. As $c \to 1/4$, the stagnation points move off towards infinity in opposite directions. The point vortex pair is stationary when $c = 1/4$.

References

[1] W.M. Hicks, On the steady motion and small vibrations of a hollow vortex, Philos. Trans. R. Soc. Lond. 175 (1884) 161–195.
[2] J.H. Michell, On the theory of free stream lines, Philos. Trans. R. Soc. Lond. 181 (1890) 389–431.
[3] H.C. Pocklington, The configuration of a pair of equal and opposite hollow straight vortices of finite cross-section moving steadily through fluid, Philos. Trans. R. Soc. Lond. 8 (1894) 178–187.
[4] P.G. Saffman, Vortex Dynamics, Cambridge University Press, Cambridge, 1992.
[5] D.G. Crowdy, C.C. Green, Analytical solutions for von Kármán streets of hollow vortices, Phys. Fluids 23 (2011) 126602.
[6] D.G. Crowdy, J. Roenby, Hollow vortices, capillary water waves and double quadrature domains, Fluid Dynam. Res. 46 (2014) 031424.
[7] D.G. Crowdy, S.G. Llewellyn Smith, D.V. Freilich, Translating hollow vortex pairs, Eur. J. Mech. B Fluids 37 (2013) 180–186.
[8] A.R. Elcrat, L. Zannetti, Models for inviscid wakes past a normal plate, J. Fluid Mech. 708 (2012) 377–396.
[9] S.G. Llewellyn Smith, D.G. Crowdy, Structure and stability of hollow vortex equilibria, J. Fluid Mech. 691 (2012) 178–200.
[10] H. Telib, L. Zannetti, Hollow wakes past arbitrarily shaped obstacles, J. Fluid Mech. 669 (2011) 214–224.
[11] L. Zannetti, D. Lasagna, Hollow vortices and wakes past Chaplygin cusps, Eur. J. Mech. B Fluids 38 (2013) 78–84.
[12] G. Giannakidis, Prandtl–Batchelor flow in a channel, Phys. Fluids 5 (1993) 863.
[13] G.R. Baker, P.G. Saffman, J.S. Sheffield, Structure of a linear array of hollow vortices of finite cross-section, J. Fluid Mech. 74 (1976) 469–476.
[14] D.G. Crowdy, Geometric function theory: a modern view of a classical subject, Nonlinearity 21 (2008) 205–219.
[15] D.G. Crowdy, Conformal slit maps in applied mathematics, ANZIAM J. 53 (2012) 171–189.
[16] D.G. Crowdy, J.S. Marshall, Conformal mappings between canonical multiply connected domains, Comput. Methods Funct. Theory 6 (2006) 59–76.
[17] C.C. Green, Mathematical techniques for free boundary problems with multiple boundaries (Ph.D. thesis), Imperial College London, 2013.
[18] K.C. Stewart, C.L. Niebel, S. Jung, P.P. Vlachos, The decay of confined vortex rings, Exp. Fluids 53 (2012) 163–171.
[19] Y. Bazilevs, J.C. del Alamo, J.D. Humphrey, From imaging to prediction: emerging non-invasive methods in pediatric cardiology, Prog. Pediatr. Cardiol. 30 (2010) 81–89.
[20] P.P. Sengupta, G. Pedrizzetti, P.J. Kilner, A. Kheradvar, T. Ebbers, G. Tonti, A.G. Fraser, J. Narula, Emerging trends in cardiovascular flow visualization, J. Am. Coll. Cardiol. Img. 5 (3) (2012) 305–316.
[21] H.F. Baker, Abelian Functions: Abel's Theorem and the Allied Theory of Theta Functions, Cambridge University Press, Cambridge, 1897.
[22] L. Rosenhead, The Kármán street of vortices in a channel of finite breadth, Philos. Trans. R. Soc. Lond. 228 (1929) 275–329.
[23] D.G. Crowdy, A.S. Fokas, C.C. Green, Conformal mappings to multiply connected polycircular arc domains, Comput. Methods Funct. Theory 11 (2) (2011) 685–706.
[24] K. Ardalan, D.I. Meiron, D.I. Pullin, Steady compressible vortex flows: the hollow-core vortex array, J. Fluid Mech. 301 (1995) 1–17.
[25] P. Luzzatto-Fegiz, C.H.K. Williamson, Stability of conservative flows and new steady-fluid solutions from bifurcation diagrams exploiting a variational argument, Phys. Rev. Lett. 104 (2010) 044504.